



# Hole mobilities of thermally polymerized triaryldiamine derivatives and their application as hole-transport materials in organic light-emitting diodes (OLEDs)

Chi-Yen Lin<sup>a</sup>, You-Ming Chen<sup>a</sup>, Hsiao-Fan Chen<sup>a</sup>, Fu-Chuan Fang<sup>a</sup>, Yu-Cheng Lin<sup>b</sup>, Wen-Yi Hung<sup>b,\*</sup>, Ken-Tsung Wong<sup>a,\*</sup>, Raymond C. Kwong<sup>c</sup>, Sean C. Xia<sup>c</sup>

<sup>a</sup> Department of Chemistry, National Taiwan University, Taipei 106, Taiwan, ROC

<sup>b</sup> Institute of Optoelectronic Sciences, National Taiwan Ocean University, Keelung 202, Taiwan, ROC

<sup>c</sup> Universal Display Corporation, 375 Phillips Blvd, Ewing, NJ 08618, USA

## ARTICLE INFO

### Article history:

Received 21 August 2008

Received in revised form 5 November 2008

Accepted 7 November 2008

Available online 18 November 2008

### PACS:

73.50.-h

73.61.Ph

78.30.Jw

78.55.Kz

78.60.Fi

78.66.Qn

### Keywords:

Solution process

Thermal polymerization

Time-of-flight (TOF)

Hole mobility

## ABSTRACT

This paper describes the synthesis of three triaryldiamine derivatives presenting two thermally polymerizable trifluorovinyl ether groups that can be polymerized through thermal curing to form perfluorocyclobutyl (PFCB) polymers. These PFCB polymers, studied using time-of-flight techniques for the first time, exhibited remarkable non-dispersive hole-transport properties, with values of  $\mu_h$  of ca.  $10^{-4} \text{ cm}^2 \text{ V}^{-1} \text{ s}^{-1}$ . When we employed these thermally polymerized polymers as hole-transport layers (HTLs) in electroluminescence devices containing tris(8-hydroxyquinolate) aluminum ( $\text{Alq}_3$ ) as the emission layer, we obtained high current densities (ca.  $3400 \text{ mA cm}^{-2}$ ), impressive brightnesses ( $5 \times 10^4 \text{ cd m}^{-2}$ ), and high external quantum efficiencies (EQEs = 1.43%). These devices exhibited the same turn-on voltage, but higher EQEs, relative to those incorporating the vacuum-processed model compound  $N,N'$ -di(1-naphthyl)- $N,N'$ -diphenylbenzidine ( $\alpha$ -NPD) (EQE = 1.37%) as the HTL under the same device structure.

© 2008 Elsevier B.V. All rights reserved.

## 1. Introduction

Organic and polymer light-emitting diodes are promising devices for use in future lighting and display applications because of their low power consumption, light weight, fast response, and wide viewing angle [1,2]. To increase their efficiency, most organic light-emitting diodes (OLEDs) are configured with a variety of functional materials into a multilayer structure—fabricated through succes-

sive vacuum deposition of small molecules—and then covered by a metal cathode. It is generally inherently difficult to form polymer-based OLEDs in multilayer structures through solution-processing techniques, such as spin-coating, because of solvent erosion of the previously deposited layers during spin-coating [3]. One of the most promising approaches toward achieving purely solution-processed multiple-layer polymer-based OLEDs is utilizing soluble precursor materials to produce insoluble polymer networks through polymerization and/or cross-linking reactions. This strategy allows the sequential deposition of various functional layers [4,5]. The flexibility of using the chemical modifications of a wide variety of materials

\* Corresponding authors. Tel.: +886 2 33661665; fax: +886 2 33661667.  
E-mail addresses: [wenhung@mail.ntou.edu.tw](mailto:wenhung@mail.ntou.edu.tw) (W.-Y. Hung), [kenwong@ntu.edu.tw](mailto:kenwong@ntu.edu.tw) (K.-T. Wong).

possessing various functional moieties—such as siloxan [6–9], norbornene [10,11], oxetane [4,5], vinyl [12,13], and trifluorovinyl ether [14–18] units—as polymerizable groups under UV irradiation or thermal curing allows the construction of copolymers in nearly any designated composition. For example, trifluorovinyl ether (TFVE)-containing compounds are useful as reactive monomers that undergo thermal cyclopolymerization to afford a new class of thermally stable perfluorocyclobutane (PFCB) polymers [19–21]. Taking advantage of this strategy, PFCB-based hole-transport materials have been developed to increase the efficiency of OLED devices [22–28]. This superior performance is ascribed mainly to the homogeneous surface morphology of the thermally treated thin films, as probed using atomic force microscopy (AFM). Nevertheless, to the best of our knowledge, the intrinsic charge transporting characteristic, one of the most critical factors in optoelectronic devices, of PFCB-based hole-transport materials has not been reported previously. In this paper, we report the synthesis, characterization, and application of three triaryldiamine derivatives attached to two thermally polymerizable trifluorovinyl ether (TFVE) groups that can be polymerized through thermal curing to form PFCB polymers. More importantly, we have used time-of-flight (TOF) techniques to study the hole-transport properties of these polymers. We have found that PFCB-based polymers possess remarkable hole-transport properties, with values of  $\mu_h$  of ca.  $10^{-4} \text{ cm}^2 \text{ V}^{-1} \text{ s}^{-1}$ . These thermally polymerized polymers are useful as hole-transport layers (HTLs) in electroluminescence (EL) applications, as evidenced by the high external quantum efficiency of 1.43% achieved when employing one such system with tris(8-hydroxyquinolate) aluminum (Alq<sub>3</sub>) as the emission layer.

## 2. Experimental

### 2.1. Synthesis

**Compound 5:** Compound **4** (5.08 g, 10 mmol), *N*-phenyl-1-naphthylamine (4.39 g, 20 mmol), Pd(OAc)<sub>2</sub> (67 mg, 0.3 mmol), and sodium *tert*-butoxide (7.68 g, 80 mmol) were dissolved in toluene (100 mL) and then tri-*tert*-butylphosphine (6 mL, 0.05 M in toluene, 0.3 mmol) was added. The mixture was heated under reflux under argon for 72 h and then quenched with water. The solution was partitioned between ethyl acetate and brine. The combined organic extracts were dried (MgSO<sub>4</sub>) and concentrated. The resulting solid was washed with hexane to afford a yellow product (6.41 g, 82%). M.p. 254–255 °C. IR (KBr)  $\nu$  3544 (w), 3055 (w), 1609 (m), 1592 (s), 1573 (m), 1507 (s), 1489 (s), 1464 (s), 1434 (m), 1392 (m), 1302 (m), 1269 (s), 1172 (m), 1015 (m) cm<sup>-1</sup>. <sup>1</sup>H NMR (DMSO-*d*<sub>6</sub>, 400 MHz):  $\delta$  9.29 (s, 2H), 7.97 (d, *J* = 8.0 Hz, 2H), 7.84 (d, *J* = 8.4 Hz, 2H), 7.76 (d, *J* = 8.4 Hz, 2H), 7.56–7.48 (m, 6H), 7.37 (t, *J* = 7.4 Hz, 2H), 7.28 (d, *J* = 7.2 Hz, 2H), 7.16 (t, *J* = 7.6 Hz, 4H), 6.92–6.84 (m, 8H), 6.78 (s, 2H), 6.51 (d, *J* = 8.8 Hz, 4H), 6.41 (d, *J* = 8.4 Hz, 4H). <sup>13</sup>C NMR (DMSO-*d*<sub>6</sub>, 100 MHz):  $\delta$  155.5, 152.2, 147.5, 146.5, 142.6, 135.3, 134.7, 132.9, 130.1, 129.1, 128.4, 128.2, 126.6, 126.4, 126.3, 126.1, 123.4, 121.6, 121.1, 120.4, 120.2, 118.8,

114.6, 63.0. MS (FAB<sup>+</sup>, *m/z*) 785 (100), 784 (65), 154 (70), 136 (65), 57 (65). HRMS (FAB<sup>+</sup>, [M+H]<sup>+</sup>) Calcd. C<sub>57</sub>H<sub>41</sub>N<sub>2</sub>O<sub>2</sub> 785.3170, found 785.3165.

**Compound 6:** A mixture of **5** (2.93 g, 3.73 mmol) and triethylamine (3 mL, 21.6 mmol) in dry dichloromethane (260 mL) was cooled to –10 °C. Trifluoromethanesulfonic anhydride (1.9 mL, 11.2 mmol) in dry dichloromethane (90 mL) was added dropwise and then the reaction mixture was warmed to room temperature and stirred for 16 h. The reaction was quenched by pouring the mixture into ice water. The organic layer was separated and the aqueous phase was extracted twice with dichloromethane. The combined organic extracts were washed with saturated NaHCO<sub>3</sub> solution and brine and then dried (MgSO<sub>4</sub>). The solvents were evaporated and the resulting residue was purified through re-precipitation from dichloromethane and methanol to afford a yellow product (3.18 g, 81%). M.p. 136–138 °C. IR (KBr)  $\nu$  3059 (w), 1609 (m), 1592 (m), 1573 (m), 1494 (s), 1468 (s), 1455 (m), 1426 (s), 1392 (m), 1271 (m), 1249 (m), 1212 (s), 1140 (s), 884 (m), 774 (m) cm<sup>-1</sup>. <sup>1</sup>H NMR (DMSO-*d*<sub>6</sub>, 400 MHz):  $\delta$  7.96 (d, *J* = 8.4 Hz, 2H), 7.85 (d, *J* = 8.0 Hz, 2H), 7.72 (d, *J* = 8.0 Hz, 2H), 7.62 (d, *J* = 8.4 Hz, 2H), 7.53–7.46 (m, 4H), 7.37–7.27 (m, 8H), 7.15 (t, *J* = 7.6 Hz, 4H), 7.00 (d, *J* = 8.4 Hz, 4H), 6.92–6.89 (m, 4H), 6.84 (d, *J* = 8.4 Hz, 6H). <sup>13</sup>C NMR (DMSO-*d*<sub>6</sub>, 100 MHz):  $\delta$  149.9, 147.7, 147.2, 146.9, 145.0, 142.3, 134.7, 132.8, 129.9, 129.3, 129.0, 128.4, 126.7, 126.5, 126.4, 126.3, 126.0, 123.2, 121.8, 121.3, 121.1, 120.8, 119.6, 118.3, 116.4, 63.6. MS (FAB<sup>+</sup>, *m/z*) 1048 (100), 916 (15), 690 (20), 218 (40), 217 (35). HRMS (FAB<sup>+</sup>, M<sup>+</sup>) Calcd. C<sub>59</sub>H<sub>38</sub>F<sub>6</sub>N<sub>2</sub>O<sub>6</sub>S<sub>2</sub> 1048.2075, found 1048.2076.

**TFVE1:** **1** (380 mg, 0.87 mmol), **2** (515 mg, 2.18 mmol), Pd(OAc)<sub>2</sub> (10 mg, 0.04 mmol), and sodium *tert*-butoxide (210 mg, 2.18 mmol) were dissolved in toluene (10 mL) and then tri-*tert*-butyl phosphine (1.6 mL, 0.05 M in toluene, 0.08 mmol) was added. The mixture was heated under reflux under argon for 24 h and then quenched with water. The solvent was evaporated and then the reaction mixture was extracted with dichloromethane and dried (MgSO<sub>4</sub>). The crude product was purified through column chromatography (SiO<sub>2</sub>; EtOAc/hexane, 1:15) to afford **TFVE1** (485 mg, 72%) as a white solid. IR (KBr)  $\nu$  3046 (w), 1600 (w), 1497 (s), 1460 (w), 1397 (m), 1311 (m), 1274 (s), 1192 (m), 1159 (m), 1136 (m) cm<sup>-1</sup>. <sup>1</sup>H NMR (acetone-*d*<sub>6</sub>, 400 MHz):  $\delta$  7.98 (d, *J* = 8.0 Hz, 2H), 7.94 (d, *J* = 8.0 Hz, 2H), 7.89 (d, *J* = 8.0 Hz, 2H), 7.55 (t, *J* = 8.0 Hz, 2H), 7.52–7.45 (m, 6H), 7.43–7.36 (m, 4H), 7.14–7.07 (m, 8H), 7.00 (d, *J* = 8.0 Hz, 4H). <sup>13</sup>C NMR (acetone-*d*<sub>6</sub>, 100 MHz):  $\delta$  148.0, 146.3, 143.8, 136.2, 134.5, 131.8, 129.3, 127.9, 127.8, 127.6, 127.3, 127.2, 127.0, 124.5, 124.2, 122.3, 117.6. <sup>19</sup>F NMR (acetone-*d*<sub>6</sub>, 376 MHz):  $\delta$  –117.1 (dd, *J* = 99.6, 55.6 Hz, 2F), –124.3 (dd, *J* = 108.3, 99.3 Hz, 2F), 130.6 (dd, *J* = 108.3, 56.4 Hz, 2F). MS (FAB<sup>+</sup>, *m/z*) 780 (100), 467 (25), 217 (35). HRMS (FAB<sup>+</sup>, M<sup>+</sup>) Calcd. C<sub>47</sub>H<sub>28</sub>N<sub>4</sub> 780.2211, found 780.2208.

**TFVE2:** A flask containing **3** (2.46 g, 4.88 mmol), 1-aminonaphthalene (2.09 g, 14.6 mmol), Pd<sub>2</sub>(dba)<sub>3</sub> (224 mg, 0.25 mmol), and sodium *tert*-butoxide (1.41 g, 14.7 mmol) was evacuated and recharged with argon, then dry toluene (30 mL) and tri-*tert*-butylphosphine (9.8 mL,

0.05 M in toluene, 0.49 mmol) were added. The mixture was heated under reflux for 48 h and then cooled to room temperature. The mixture was filtered through a short path of Celite and then washed with dichloromethane, and the filtrate was extracted with dichloromethane and dried (MgSO<sub>4</sub>). The solvent was partially removed using a rotary evaporator and then hexane (30 mL) was added to give a yellow solid that was collected through filtration and washed with hexane. The crude solid (1.9 g, 3.02 mmol) was combined with Pd(OAc)<sub>2</sub> (34 mg, 0.15 mmol), **2** (1.91 g, 7.5 mmol), and sodium *tert*-butoxide (1.44 g, 15 mmol) and then dry toluene (40 mL) and tri-*tert*-butylphosphine (6 mL, 0.05 M in toluene, 0.3 mmol) were added. The mixture was filtered through a short path of Celite and washed with ethyl acetate, and the filtrate was extracted with ethyl acetate and dried (MgSO<sub>4</sub>). The solvent was removed using a rotary evaporator to give a crude product, which was purified through column chromatography (SiO<sub>2</sub>; EtOAc:hexane, 1:20) to afford **TFVE2** (2.3 g, 49% over two steps) as a yellow solid. IR (KBr)  $\nu$  3048 (m), 2917 (w), 2869 (w), 1831 (w), 1604 (m), 1573 (w), 1499 (s), 1465 (s), 1440 (m), 1392 (m), 1311 (s), 1274 (s), 1192 (s), 1164 (m), 1137 (s), 1019 (w), 816 (m), 798 (m), 772 (m) cm<sup>-1</sup>. <sup>1</sup>H NMR (CDCl<sub>3</sub>, 400 MHz):  $\delta$  7.94 (d, *J* = 4.2 Hz, 2H), 7.83 (t, *J* = 8.8 Hz, 4H), 7.56 (d, *J* = 4.6 Hz, 2H), 7.49 (t, *J* = 8 Hz, 4H), 7.35 (t, *J* = 6.8 Hz, 2H), 7.28 (d, *J* = 3.4 Hz, 2H), 7.06 (d, *J* = 4.6 Hz, 4H), 6.96 (m, 8H), 6.85 (d, *J* = 4 Hz, 4H), 6.74 (d, *J* = 4.2 Hz, 4H), 2.21 (s, 6H). <sup>13</sup>C NMR (CDCl<sub>3</sub>, 100 MHz):  $\delta$  152.5, 149.6, 147.4, 145.7, 143.3, 142.6, 135.8, 135.5, 134, 130.6, 128.6, 128.5, 127.7, 126.7, 126.6, 126.4, 126.2, 123.9, 123.4, 121, 120.4, 119.5, 116.8, 64.6, 20.2. <sup>19</sup>F NMR (CDCl<sub>3</sub>, 376 MHz):  $\delta$  -115.8 (dd, *J* = 98.9, 56.4 Hz, 2F), -123.0 (dd, *J* = 108.3, 99.3 Hz, 2F), -129.2 (dd, *J* = 107.5, 55.6 Hz, 2F). MS (FAB<sup>+</sup>, *m/z*) 973 (100), 972 (35), 881 (15), 659 (30), 217 (20). HRMS (FAB<sup>+</sup>, [M+H]<sup>+</sup>) Calcd. C<sub>63</sub>H<sub>43</sub>O<sub>2</sub>N<sub>2</sub>F<sub>6</sub>: 973.3230, found: 973.3238.

**TFVE3: 6** (2.1 g, 2 mmol), **7** (1.44 g, 4.8 mmol), and Pd(PPh<sub>3</sub>)<sub>4</sub> (0.1 g, 0.086 mmol) were dissolved in 1,4-dioxane (25 mL) and then sodium carbonate (10 mL, 2 M in H<sub>2</sub>O) was added. The mixture was heated under reflux under Ar for 72 h and then quenched with water, extracted with dichloromethane, and dried (MgSO<sub>4</sub>). The crude product was purified through column chromatography (SiO<sub>2</sub>; toluene/hexane, 1:3) to afford **TFVE3** (1.2 g, 55%) as a yellow solid. IR (KBr)  $\nu$  3056 (w), 2942 (w), 1592 (m), 1574 (m), 1492 (s), 1465 (m), 1429 (m), 1387 (w), 1310 (m), 1273 (s), 1197 (m), 1175 (m), 1138 (m) cm<sup>-1</sup>. <sup>1</sup>H NMR (DMSO-*d*<sub>6</sub>, 400 MHz):  $\delta$  7.96 (d, *J* = 7.6 Hz, 2H), 7.84 (d, *J* = 8.0 Hz, 2H), 7.76 (d, *J* = 8.4 Hz, 2H), 7.64 (t, *J* = 8.0 Hz, 6H), 7.53–7.46 (m, 4H), 7.40–7.36 (m, 10H), 7.30 (d, *J* = 6.8 Hz, 2H), 7.18 (t, *J* = 8.0 Hz, 4H), 6.93–6.84 (m, 14H). <sup>13</sup>C NMR (DMSO-*d*<sub>6</sub>, 100 MHz):  $\delta$  153.4, 150.8, 147.3, 146.7, 143.9, 142.4, 137.0, 136.4, 134.7, 133.0, 129.9, 129.0, 128.7, 128.4, 128.2, 127.7, 126.5, 126.4, 126.2, 126.0, 123.3, 121.8, 121.4, 120.6, 120.5, 118.4, 115.9, 63.8. <sup>19</sup>F NMR (DMSO-*d*<sub>6</sub>, 376 MHz):  $\delta$  -117.8 (dd, *J* = 96.3, 54.9 Hz, 2F), -125.6 (dd, *J* = 107.5, 96.6 Hz, 2F), -133.6 (dd, *J* = 107.5, 55.6 Hz, 2F). MS (FAB<sup>+</sup>, *m/z*) 1097 (100), 880 (15), 217 (35). HRMS ([M+H]<sup>+</sup>, FAB<sup>+</sup>) Calcd. C<sub>73</sub>H<sub>47</sub>F<sub>6</sub>N<sub>2</sub>O<sub>2</sub> 1097.3543, found 1097.3534.

## 2.2. Time-of-flight (TOF) mobility measurements

In the TOF method, a sheet of carriers is created near one of the contacts using a short laser pulse (nitrogen pulse laser). The sample is illuminated from the indium tin oxide (ITO) side to generate a sheet of charge carriers in the organic layer. Under the influence of an applied electric field, these carriers drift toward the counter electrode (Ag), resulting in a transient current through the sample. When the carriers reach the counter electrode, the current drops to zero; the point at which this happens corresponds to the transit time of the carriers (*t*<sub>T</sub>). Depending on the polarity of the applied bias, selected photogenerated carriers (holes or electrons) are swept across the sample thickness *D*; the applied electric field *E* is then equal to *V/D*, and the carrier mobility ( $\mu$ ) is given by *D/(t*<sub>T</sub>*E)*.

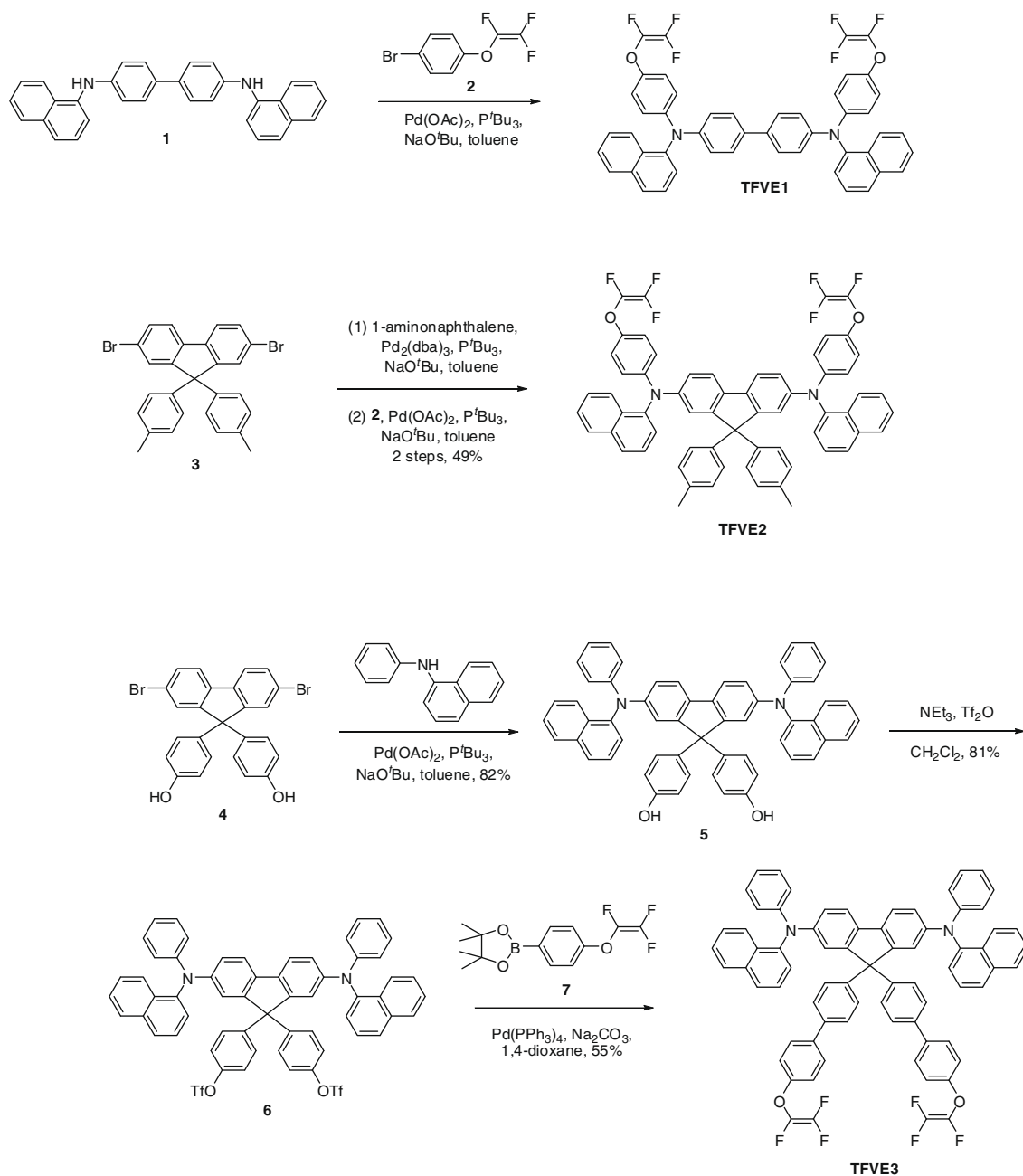
## 2.3. OLED device

The OLEDs were fabricated on ITO sheets having a resistance of 15  $\Omega/\square$ . The substrates were washed sequentially with isopropyl alcohol, acetone, and methanol in an ultrasonic bath, followed by UV-ozone treatment prior to use. A hole injecting poly(ethylene dioxythiophene): polystyrene sulfonate (PEDOT:PSS) layer was spin-coated onto the substrates and dried at 130 °C for 30 min to remove residual water. The substrates were transferred to a N<sub>2</sub>-filled glove box. The crosslinkable **TFVE1–3** monomers (1.2 wt%) were dissolved in THF, dip-coated atop the PEDOT:PSS layer to yield ca. 50-nm-thick films, and then cured at 230 °C for 30 min to promote crosslinking. To prepare the emissive and electron transport layer, a 60-nm layer of Alq<sub>3</sub> was vacuum-deposited on top of the spin-coated HTL. The devices were then completed through thermal evaporation of the back electrode [LiF (0.5 nm)/Ag (100 nm)] through a shadow mask. All evaporations were performed under a vacuum of less than 10<sup>-6</sup> torr. Each device pixel had an active area of 0.25 $\pi$  mm<sup>2</sup>. The current–voltage–brightness (*I–V–L*) characteristics of the devices were measured simultaneously using a Keithley 6430 source meter and a Keithley 6487 picoammeter equipped with a calibration Si-photodiode. EL spectra were measured using an ocean optics spectrometer.

## 3. Results and discussion

### 3.1. Materials

**Scheme 1** depicts the syntheses of monomers **TFVE1–3**, which were derivatives of the well-established hole-transporting material *N,N'*-di(1-naphthyl)-*N,N'*-diphenylbenzidine ( $\alpha$ -NPD). **TFVE1**, possessing two trifluorovinyl ether (TFVE) groups linked to the terminal phenylene rings of  $\alpha$ -NPD, was synthesized in an isolated yield of 72% through Pd-catalyzed amination of diamine **1** and compound **2** [20]. **TFVE2**, which had similar structural features to the terminal groups of **TFVE1**, but with the diarylamino groups attached to a coplanar rigid core (fluorene) to modulate the electronic properties, was synthesized through the reaction of 2,7-dibromo-9,9-ditolylfluorene (**3**) [29] with



**Scheme 1.** Synthesis of trifluorovinyl ether-functionalized monomers **TFVE1–3**.

1-aminonaphthalene in the presence of a catalytic amount of  $\text{Pd}_2(\text{dba})_3$  to furnish an aminated crude product that was subsequently subjected to Pd-catalyzed amination with compound **2** (49% yield over two steps). Without structural perturbation of the active chromophore, the two TFVE groups of **TFVE3** were introduced onto the peripheral biphenyl substituents of the central fluorene unit. The amination of compound **4** [30] with *N*-phenyl-1-naphthylamine in the presence of a catalytic amount of  $\text{Pd(OAc)}_2$  and tri-*tert*-butyl phosphine gave compound **5** in 82% yield. The treatment of the phenol groups in **5** with trifluoromethane-

sulfonic anhydride afforded the disulfonate **6** in 81% yield. **TFVE3** was then obtained in 55% yield after Suzuki coupling of the boronic ester **7** [15] and compound **6**.

### 3.2. Physical properties

The morphological properties of the monomers **TFVE1–3** were investigated using differential scanning calorimetry (DSC). The introduction of two TFVE groups had a pronounced effect on the morphology. As indicated in Fig. 1, no evident glass transition could be detected for **TFVE1**; in-

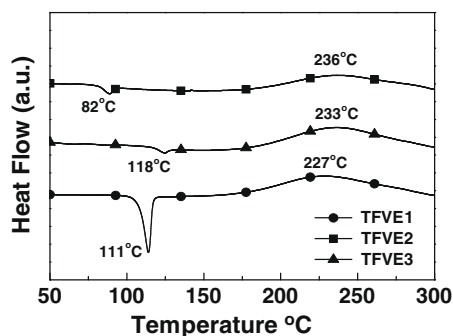


Fig. 1. DSC analyses of the thermally polymerizable monomers **TFVE1–3**.

stead, we observed an endothermic peak centered at 111 °C, which corresponded to the melting point of **TFVE1**. The increased molecular rigidity of **TFVE2** led to a distinct glass transition temperature ( $T_g$ ) detected at 82 °C, which remained significantly lower than that of its parent compound (127 °C) [29]. **TFVE3**, with its two TFVE groups attached to the peripheral biphenyl substituents of the central fluorene unit, possesses a value of  $T_g$  of 118 °C. The exothermic peaks of **TFVE1–3** at ca. 230 °C in the DSC traces correspond to their thermal polymerizations, consistent with the previously reported polymerization temperatures of TFVE groups [14–28]. The three TFVE monomers were soluble in common organic solvents, such as chloroform, tetrahydrofuran (THF), and toluene. After dip-coating solutions of the TFVEs in THF onto ITO substrates, the films were baked at 100 °C for 30 min to remove any residual solvent. Atomic force microscopy (AFM) reveals that the films prepared through this dip-coating process had smooth surfaces with no obvious crystallization, pinholes, or cracks (Fig. 2). After curing at 230 °C for 60 min, the films of the PFCB polymers became

insoluble in most organic solvents. The AFM images of these PFCB polymer films reveal some clusters formed after thermal polymerization at high temperature.

Fig. 3a displays UV–vis absorption and photoluminescence spectra of the thin films of vacuum-deposited  $\alpha$ -NPD and **TFVE1–3** after thermal polymerization. The absorption spectrum ( $\lambda_{\text{max}} = 344$  nm) of **TFVE1** polymer matches well with that of  $\alpha$ -NPD, whereas polymers of **TFVE2** and **TFVE3** exhibit red-shifted absorption maxima (by ca. 40 nm), due to the coplanar structure of their cores. There were no significant changes in the absorption spectra of **TFVE1–3** after the treatment at high temperature (Fig. 3b and c). In contrast to their electronic transitions, the emission spectra of the thermally polymerized thin films of **TFVE1–3** exhibit slightly red-shifted maxima with broader half-widths of the emission peaks, relative to that of the  $\alpha$ -NPD thin film and the thin films of **TFVE1–3** prior to thermal polymerization. These results contrast those from a previous report by Jen et al., where a thin film of a *N,N'*-di(3-methylphenyl)-*N,N'*-diphenylbenzidine (TPD)-based PFCB polymer exhibited an obviously red-shifted emission maximum relative to that of its monomer film as a result of strong aggregation and excimer emission [22–28]. The observed limited red shifts in the emission of **TFVE1–3** polymers and their long-wavelength tails could be attributable to the changes in the dielectric environments upon thermal treatment. The chromophores surrounded by TFVE moieties in the monomeric states should behave differently from those in the polymeric forms, in which the TFVE groups have been converted into PFCB moieties. Nevertheless, we cannot exclude the possibility of weak interchromophore interactions leading to long-wavelength emission regions in the polymer films after high-temperature thermal polymerization.

To characterize the hole transport in these thermally polymerized **TFVE1–3** polymers and to quantify their mobilities, we used time-of-flight (TOF) techniques [31]

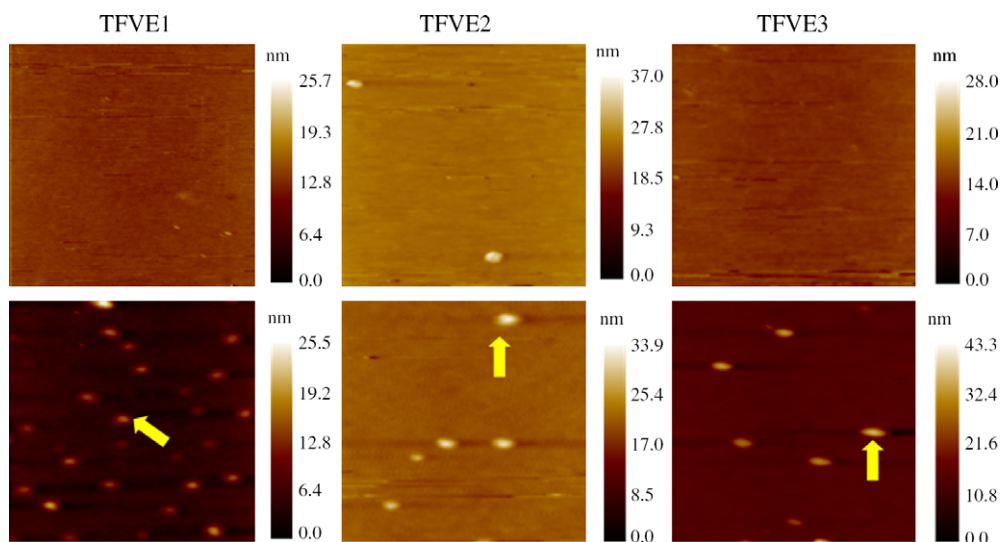
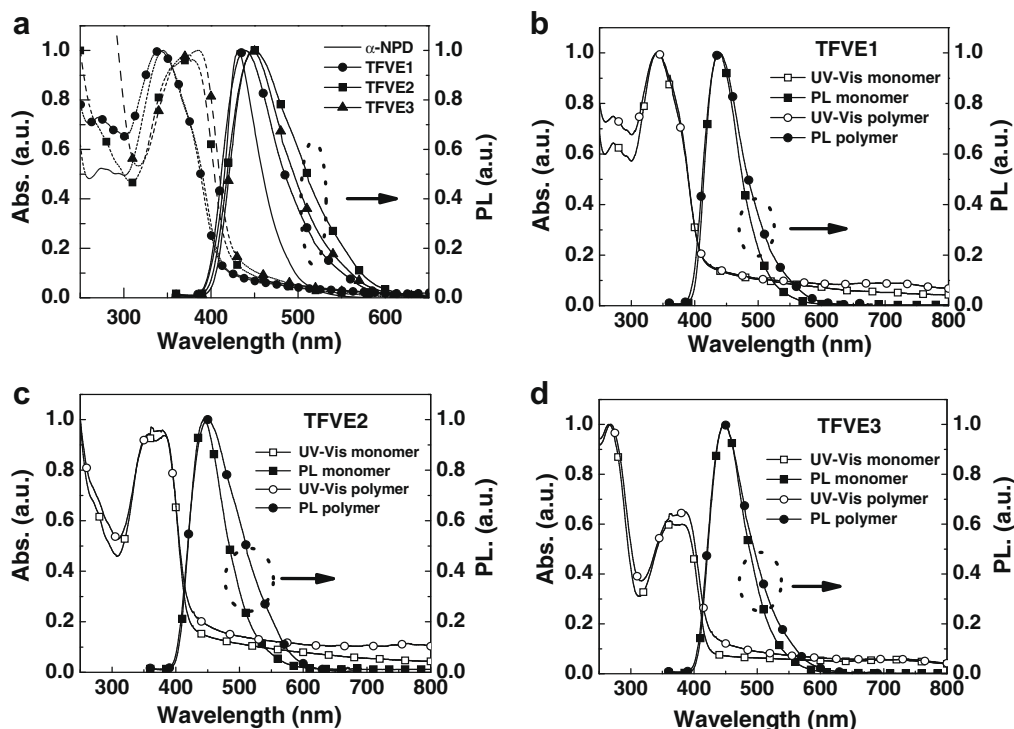


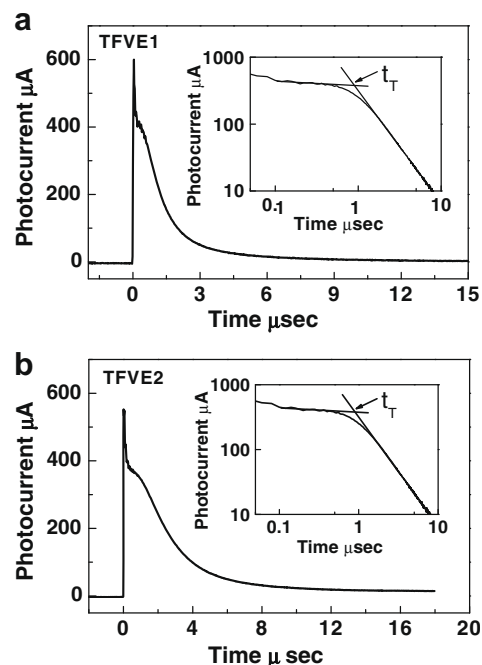
Fig. 2. AFM images ( $5 \times 5 \mu\text{m}$ ) of **TFVE1–3** thin films before (top) and after (bottom) thermal polymerization. The indicated clusters with heights of **TFVE1** (11 nm), **TFVE2** (13 nm), and **TFVE3** (16 nm), respectively.



**Fig. 3.** (a) UV-vis absorption and photoluminescence spectra of thin films of thermally polymerized TFVE1–3 and vacuum-deposited  $\alpha$ -NPD and (b–d) comparisons of photophysical properties of TFVE1–3 thin films before (monomers) and after thermal polymerization (polymers).

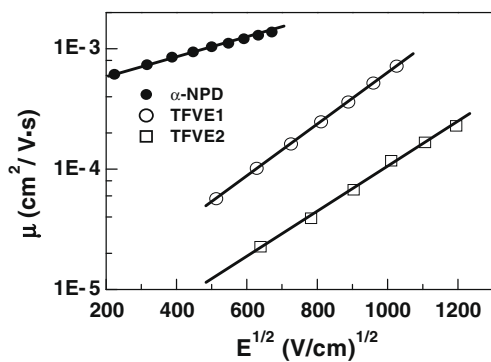
to measure the charge carrier mobility. This technique has been successfully applied to investigate the charge transport behavior of a wide range of polymers and small molecules, but it has not been applied previously to measure the charge mobility of any thermal polymerized and/or cross-linked polymers. TOF samples were prepared by dissolving appropriate weight ratios (up to 25 wt%) of the monomers TFVE1 and TFVE2 in THF and then dip-coating the solutions onto an ITO substrate within a glove box. For TFVE3, however, poor solubility in THF meant that we could not obtain a solution of sufficiently high concentration to yield a sample that was thick enough for TOF measurement. We were able to control the film thicknesses by varying the solution concentrations and the dip-coating conditions; the films were subsequently dried through baking at 100 °C for 30 min to remove the residual solvent and then curing at 230 °C for 60 min to form the polymers. We used a Dektak surface profilometer to measure the thicknesses of the TFVE1 (ca. 760 nm) and TFVE2 (ca. 500 nm) polymer films. The samples were then completed through thermal deposition of the back electrode [Ag (100 nm)] through a shadow mask.

Fig. 4 displays the TOF transients of the TFVE1 and TFVE2 polymer films. Distinctive plateaus are visible in the typical TOF transient photocurrents, indicating the non-dispersive transport behavior of the TFVE1 and TFVE2 polymers toward holes. We estimated the carrier transit times  $t_T$  from the asymptotes of the log-log plots (insets to Fig. 4); from these values, we deduced the hole mobilities ( $\mu$ ) using the relation  $\mu = d/(Et_T)$ , where  $E$  and  $d$  are the applied electric field and the thickness of the organic film,



**Fig. 4.** Representative TOF transients for polymer films derived from (a) TFVE1 (at  $E = 5.3 \times 10^5$  cm V<sup>-1</sup>) and (b) TFVE2 (at  $E = 6.1 \times 10^5$  cm V<sup>-1</sup>) at room temperature. The insets present double-logarithmic plots of the data.

respectively. Fig. 5 presents the room-temperature hole mobilities of the model compound  $\alpha$ -NPD and of the



**Fig. 5.** Plots of hole mobilities vs.  $E^{1/2}$  for the thermally polymerized films of **TFVE1** and **TFVE2** and of a film of the model compound  $\alpha$ -NPD obtained through thermal evaporation.

PFCB-based polymer films derived from **TFVE1** and **TFVE2** plotted against the square root of the applied electric field. The linear correlation follows the universal Poole–Frenkel relationship,  $\mu = \mu_0 \exp(\beta E^{1/2})$ , where  $\mu_0$  is the zero-field mobility,  $\beta$  is the Poole–Frenkel factor and  $E$  is the electric field [32]. The hole mobilities ranged from  $2 \times 10^{-5}$  to  $10^{-3}$   $\text{cm}^2 \text{V}^{-1} \text{s}^{-1}$  for fields varying from  $4 \times 10^4$  to  $1.4 \times 10^6$   $\text{V cm}^{-1}$  and the values ( $\mu_0$  and  $\beta$ ) of fitting data are summarized in Table 1.

The observed hole mobility ( $\mu_{\text{th}} = \text{ca. } 10^{-4}$   $\text{cm}^2 \text{V}^{-1} \text{s}^{-1}$ ) of the **TFVE1**-derived polymer film was about one order of magnitude lower than that of the model compound  $\alpha$ -NPD ( $\mu_{\text{th}} = 1.2 \times 10^{-3}$   $\text{cm}^2 \text{V}^{-1} \text{s}^{-1}$ ) under the same electric field ( $E = 3.6 \times 10^5$   $\text{V cm}^{-1}$ ). In addition, as indicated by its larger value of  $\beta$ , the **TFVE1**-derived polymer film exhibited a stronger electric-field-dependent hole mobility. We ascribe these phenomena to the presence of the PFCB units of the **TFVE1**-derived polymer; i.e., the more rigid structure and the larger distance and steric hindrance between neighboring chromophores increased the carrier hopping distance, thus retarding hole migration. The aggregates observed in the AFM images of the thermally treated thin films might also have been another attribute responsible for the lower hole mobility. The steric effect on hole transportation was also evident from the lower hole mobility of

**Table 1**

The values of zero-field hole mobility ( $\mu_0$ ) and Poole–Frenkel factor ( $\beta$ ) obtained by fitting the data in Fig. 5 with the Poole–Frenkel equation.

HTL	[ $\text{cm}^2 \text{V}^{-1} \text{s}^{-1}$ ]	$\beta$
$\alpha$ -NPD	$4.18 \times 10^{-4}$	$1.79 \times 10^{-3}$
<b>TFVE1</b>	$4.53 \times 10^{-6}$	$4.93 \times 10^{-3}$
<b>TFVE2</b>	$1.46 \times 10^{-6}$	$4.27 \times 10^{-3}$

**Table 2**

Device characteristics of OLEDs incorporating cross-linked **TFVE1–3** and vacuum-deposited  $\alpha$ -NPD as HTLs.

HTL	$V_{\text{on}}$ [V]	$L_{\text{max}}$ [ $\text{cd m}^{-2}$ ]	$I_{\text{max}}$ [ $\text{mA cm}^{-2}$ ]	$\eta_{\text{ext}}$ (max) [% $\text{cd A}^{-1}$ ]	$\eta_{\text{p}}$ (max) [ $\text{lm W}^{-1}$ ]
$\alpha$ -NPD	2	86,000 (11.5 V)	3500	1.36, 4.4	4
<b>TFVE1</b>	2	50,000 (14.0 V)	3400	1.43, 4.6	3.6
<b>TFVE2</b>	2	43,000 (13.5 V)	4600	1.32, 4.2	3.6
<b>TFVE3</b>	2	26,600 (14.0 V)	3900	1.32, 4.2	2.4

the **TFVE2**-derived polymer (a 9,9-ditylfluorene-based diamine) relative to that of the **TFVE1**-derived polymer (a biphenylene-based diamine) [33].

### 3.3. Device

To evaluate the performances of devices incorporating the thermally polymerized **TFVE1–3** films as HTLs, we fabricated two-layer devices having the configuration ITO/PEDOT:PSS (30 nm)/polymeric **TFVE1–3** (ca. 50 nm)/ $\text{Alq}_3$  (60 nm)/LiF (0.5 nm)/Al (100 nm). Uniform films were formed through first dip-coating the solution of **TFVE1–3** (1.2 wt% in THF) onto the pre-dried (130 °C for 30 min) PEDOT:PSS layer on an ITO substrate [34,35] and then polymerizing under thermal treatment at 230 °C for 30 min. Integrating the conductive HIL and the thermally polymerized HTL together resulted in a low driving

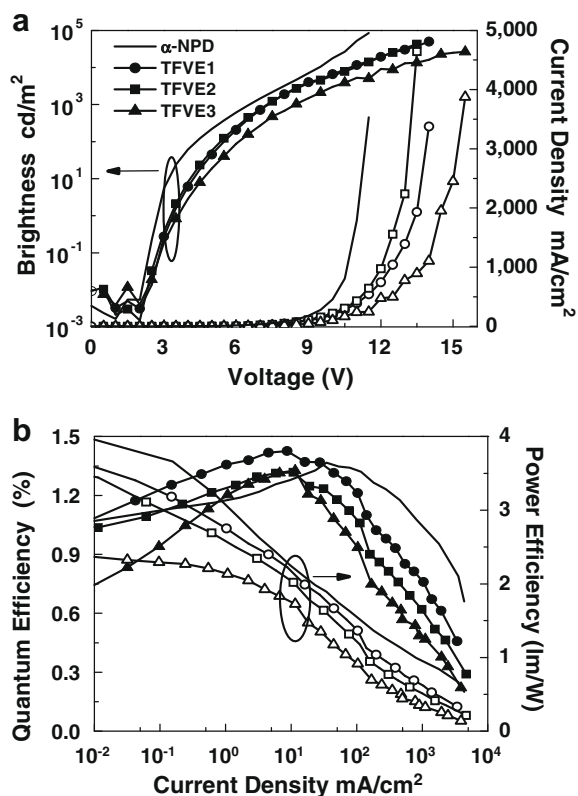


**Fig. 6.** Performances of typical two-layer devices incorporating thermally polymerized HTLs and  $\alpha$ -NPD. Plots of (a) brightness (solid symbols) and current (open symbols) vs. voltage and (b) quantum efficiency (solid symbols) and power efficiency (open symbols) vs. current.

voltage, cascade hole injection, and effective electron blocking/exciton confinement in the Alq<sub>3</sub> layer. All devices exhibited the same emission, which originated exclusively from the Alq<sub>3</sub> layer.

Table 2 and Fig. 6 summarize the EL characteristics of the OLEDs incorporating the thermally polymerized **TFVE1–3** monomers and vacuum-deposited  $\alpha$ -NPD as HTLs. These hybrid OLEDs exhibit noteworthy properties relative to those of conventional vacuum-deposited OLEDs. For example, the thermally polymerized HTLs functioned well without decreasing the device performance [10]. As indicated in Fig. 5a, the devices turned on sharply at low voltages (ca. 2 V), probably because the HOMO and LUMO energy levels of the active triaryldiamine chromophores, which remained intact before and after thermal polymerization, were matched well with those of ITO and Alq<sub>3</sub>. Among our three new thermally polymerizable HTL materials, the **TFVE1**-derived polymer exhibited the best performance. Fig. 5b indicates that the highest efficiency was achieved when using the **TFVE1**-derived polymer as the HTL: the maximum EQE was 1.43% (4.6 cd A<sup>-1</sup>) and the maximum power efficiency was 3.6 lm W<sup>-1</sup>. It is generally accepted that polymers exhibiting high morphological stability in their thin film form result in devices that can endure relatively high current densities (ca. 3400 mA cm<sup>-2</sup>) and, consequently, emit an impressive maximum brightness of nearly 5 × 10<sup>4</sup> cd m<sup>-2</sup> at ca. 14 V from the non-doped Alq<sub>3</sub>. Despite the lower hole mobility of the **TFVE1**-derived polymer films, compared with that of the vacuum-deposited model compound  $\alpha$ -NPD, the device incorporating the former as the HTL exhibited the same turn-on voltage and slightly higher EQE (1.43%) relative to that of the latter (EQE = 1.37%) under the same device structure. We attributed the higher EQE achieved in the hybrid OLED to a more balanced recombination of holes and electrons.

#### 4. Conclusions

In summary, we have synthesized and characterized three thermally polymerizable hole-transporting materials, **TFVE1–3**, derived from the parent  $\alpha$ -NPD core through the attachment of TFVE groups. The thermally polymerized monomers exhibited good thermal properties, solvent resistance, and relatively high surface smoothness. More importantly, for the first time we used TOF techniques to measure the hole-transporting characteristics of  $\alpha$ -NPD-based PFCB polymers. We observed a hole mobility of ca. 10<sup>-4</sup> cm<sup>2</sup> V<sup>-1</sup> s<sup>-1</sup> for **TFVE1**-derived polymer films, ca. one order of magnitude lower than that of the model compound  $\alpha$ -NPD (i.e., in the absence of TFVE groups) under the same electric field. We ascribe the lower mobilities of the PFCB-based polymers to their larger degrees of spatial and steric hindrance leading to blocking of carrier hopping. We fabricated hybrid OLEDs incorporating the **TFVE1**-derived polymer film as the HTL. These devices exhibited high current densities (ca. 3400 mA cm<sup>-2</sup>), impressive brightness (5 × 10<sup>4</sup> cd m<sup>-2</sup>), and high external quantum efficiency (1.43%).

#### Acknowledgement

This study was supported financially by the National Science Council of Taiwan.

#### References

- [1] C.W. Tang, S.A. VanSlyke, *Appl. Phys. Lett.* 51 (1987) 913.
- [2] A.R. Brown, R.N. Marks, K. Mackay, R.H. Friend, P.L. Burns, A.B. Holmes, *Nature (London)* 3471 (1990) 539.
- [3] B. Yan, B.J. Scott, Q. Huang, Q. Marks, *Adv. Mater.* 16 (2004) 1948.
- [4] C.D. Müller, A. Falcou, N. Reckefuss, M. Rojahn, V. Wiederhirn, P. Rudati, H. Frohne, O. Nuyken, H. Becker, K. Meerholz, *Nature (London)* 421 (2003) 829.
- [5] M.C. Gather, A. Köhnen, A. Falcou, H. Becker, K. Meerholz, *Adv. Funct. Mater.* 17 (2007) 191.
- [6] R.J.P. Corriu, D. Leclercq, *Angew. Chem., Int. Ed. Eng.* 35 (1996) 1420.
- [7] U. Schubert, N. Hüsing, A. Lorenz, *Chem. Mater.* 7 (1995) 2010.
- [8] W. Li, Q. Wang, J. Cui, H. Chou, S.E. Shaheen, G.E. Jabbour, J. Anderson, P. Lee, B. Kippelen, N. Peyghambarian, N.R. Armstrong, T.J. Marks, *Adv. Mater.* 11 (1999) 730.
- [9] J.G.C. Veinot, T.J. Marks, *Accounts Chem. Res.* 38 (2005) 632.
- [10] E. Bellmann, S.E. Shaheen, S. Thayumanavan, S. Barlow, R.H. Grubbs, S.R. Marder, B. Kippelen, N. Peyghambarian, *Chem. Mater.* 10 (1998) 1668.
- [11] A. Kimyonok, B. Domercq, A. Haldi, J.-Y. Cho, J.R. Carlise, X.-Y. Wang, L.E. Hayden, S.C. Jones, S. Barlow, S.R. Marder, B. Kippelen, M. Weck, *Chem. Mater.* 19 (2007) 5602.
- [12] A. Bacher, C.H. Erdelen, W. Paulus, H. Ringsdorf, H.-W. Schmidt, P. Schuhmacher, *Macromolecules* 32 (1999) 4551.
- [13] Y.-H. Niu, M.S. Liu, J.-W. Ka, J. Bardeker, M.T. Zin, R. Schofield, Y. Chi, A.K.-Y. Jen, *Adv. Mater.* 19 (2007) 300.
- [14] B.K. Spraul, S. Suresh, U.Y. Jin, D.W. Smith Jr., *J. Am. Chem. Soc.* 128 (2006) 7055.
- [15] B. Lim, J.-T. Hwang, J.Y. Kim, J. Ghim, D. Vak, Y.-Y. Noh, S.-H. Lee, K. Lee, A.J. Heeger, D.-Y. Kim, *Org. Lett.* 8 (2006) 4703.
- [16] B.K. Spraul, S. Suresh, S. Glaser, D. Perahia, J. Ballato, D.W. Smith Jr., *J. Am. Chem. Soc.* 126 (2004) 12772.
- [17] A.R. Neilson, S.M. Budy, J.M. Ballato, D.W. Smith Jr., *Macromolecules* 40 (2007) 9378.
- [18] J. Ghim, H.-S. Shim, B.G. Shin, J.-H. Park, J.-T. Hwang, C. Chun, S.-H. Oh, J.-J. Kim, D.-Y. Kim, *Macromolecules* 38 (2005) 8278.
- [19] J. Ji, S. Narayan-Sarathy, R.H. Neilson, J.D. Oxley, D.A. Babb, N.G. Rondan, D.W. Smith, *Macromolecules* 17 (1998) 783.
- [20] D.W. Smith, D.A. Babb, *Macromolecules* 29 (1996) 852.
- [21] D.A. Babb, B.R. Ezzell, K.S. Clement, W.F. Richey, A.P. Kennedy, *J. Polym. Sci. Part A: Polym. Chem.* 31 (1993) 3465.
- [22] Y.-H. Niu, Y.-L. Tung, Y. Chi, C.-F. Shu, J.H. Kim, B. Chen, J. Luo, A.J. Carty, A.K.-Y. Jen, *Chem. Mater.* 17 (2005) 3532.
- [23] X. Gong, D. Moses, A.J. Heeger, S. Liu, A.K.-Y. Jen, *Appl. Phys. Lett.* 83 (2003) 183.
- [24] X. Jiang, S. Liu, M.S. Liu, P. Herguth, A.K.-Y. Jen, H. Fong, M. Sarikaya, *Adv. Funct. Mater.* 12 (2002) 745.
- [25] S. Liu, X. Jiang, H. Ma, M.S. Liu, A.K.-Y. Jen, *Macromolecules* 33 (2000) 3514.
- [26] X. Jiang, M.S. Liu, A.K.-Y. Jen, *J. Appl. Phys.* 91 (2002) 10147.
- [27] Y.H. Niu, B. Chen, S. Liu, H. Yip, J. Bardecker, A.K.-Y. Jen, J. Kavitha, C.-F. Shu, Y. Chi, Y.-H. Tseng, C.-H. Chien, *Appl. Phys. Lett.* 85 (2004) 1619.
- [28] J. Zhao, J. Bardecker, A.M. Munro, M.S. Liu, Y. Niu, I.-K. Ding, J. Luo, B. Chen, A.K.-Y. Jen, D.S. Ginger, *Nano Lett.* 6 (2006) 463.
- [29] K.-T. Wong, Z.-J. Wang, Y.-Y. Chien, C.-L. Wang, *Org. Lett.* 3 (2001) 2285.
- [30] C.-H. Chou, C.-F. Shu, *Macromolecules* 35 (2002) 9673.
- [31] P.M. Borsenberger, D.S. Weiss, *Organic Photoreceptors for Imaging Systems*, Marcel Dekker, New York, 1993.
- [32] P.M. Borsenberger, L. Pautmeier, H. Bässler, *J. Chem. Phys.* 94 (1991) 5447.
- [33] Y.-L. Liao, W.-Y. Hung, T.-H. Hou, C.-Y. Lin, K.-T. Wong, *Chem. Mater.* 19 (2007) 6350.
- [34] Y. Cao, G. Yu, C. Zhang, R. Menon, A.J. Heeger, *Synth. Metal.* 87 (1997) 171.
- [35] A. Berntsen, Y. Croonen, C. Liednbaum, H. Schoo, R.-J. Visser, J. Vlegaar, P. van de Weijer, *Opt. Mater.* 9 (1998) 125.